

Hybrid multiscale coarse-graining for dynamics on complex networks

Chuansheng Shen, Hanshuang Chen, Zhonghuai Hou, and Jürgen Kurths

Citation: *Chaos* **28**, 123122 (2018); doi: 10.1063/1.5048962

View online: <https://doi.org/10.1063/1.5048962>

View Table of Contents: <http://aip.scitation.org/toc/cha/28/12>

Published by the [American Institute of Physics](#)

Articles you may be interested in

[New topological tool for multistable dynamical systems](#)

Chaos: An Interdisciplinary Journal of Nonlinear Science **28**, 111101 (2018); 10.1063/1.5062598

[Synchronization of heterogeneous oscillator populations in response to weak and strong coupling](#)

Chaos: An Interdisciplinary Journal of Nonlinear Science **28**, 123114 (2018); 10.1063/1.5049475

[Rapid time series prediction with a hardware-based reservoir computer](#)

Chaos: An Interdisciplinary Journal of Nonlinear Science **28**, 123119 (2018); 10.1063/1.5048199

[Spectral properties of complex networks](#)

Chaos: An Interdisciplinary Journal of Nonlinear Science **28**, 102101 (2018); 10.1063/1.5040897

[Reconstructing signed networks via Ising dynamics](#)

Chaos: An Interdisciplinary Journal of Nonlinear Science **28**, 123117 (2018); 10.1063/1.5053723

[Identifying the linear region based on machine learning to calculate the largest Lyapunov exponent from chaotic time series](#)

Chaos: An Interdisciplinary Journal of Nonlinear Science **28**, 123118 (2018); 10.1063/1.5065373



Don't let your writing
keep you from getting
published!

AIP | Author Services

Learn more today!

Hybrid multiscale coarse-graining for dynamics on complex networks

Chuansheng Shen,^{1,2,3} Hanshuang Chen,^{4,a)} Zhonghuai Hou,⁵ and Jürgen Kurths^{2,3}

¹*School of Mathematics and Computational Science, Anqing Normal University, Anqing 246011, China*

²*Potsdam Institute for Climate Impact Research, Potsdam 14473, Germany*

³*Department of Physics, Humboldt University, Berlin 12489, Germany*

⁴*School of Physics and Materials Science, Anhui University, Hefei 230039, China*

⁵*Hefei National Laboratory for Physical Sciences at Microscales and Department of Chemical Physics, University of Science and Technology of China, Hefei 230026, China*

(Received 19 July 2018; accepted 3 December 2018; published online 20 December 2018)

We propose a hybrid multiscale coarse-grained (HMCG) method which combines a fine Monte Carlo (MC) simulation on the part of nodes of interest with a more coarse Langevin dynamics on the rest part. We demonstrate the validity of our method by analyzing the equilibrium Ising model and the nonequilibrium susceptible-infected-susceptible model. It is found that HMCG not only works very well in reproducing the phase transitions and critical phenomena of the microscopic models, but also accelerates the evaluation of dynamics with significant computational savings compared to microscopic MC simulations directly for the whole networks. The proposed method is general and can be applied to a wide variety of networked systems just adopting appropriate microscopic simulation methods and coarse graining approaches. *Published by AIP Publishing.* <https://doi.org/10.1063/1.5048962>

Brute-force simulations for many dynamical processes on large-scale networks, such as firing activity on brain networks, epidemic spreading on human contacting networks, and information transmission on the Internet, are quite expensive. While phenomenological methods like mean-field theory may capture some macroscopic properties, they often ignore important microscopic details. Customarily, people are actually interested in the property of local part than the whole network. Under this case, a hybrid treatment with distinct coarse degrees for dynamics on networks is a promising alternative. In the present work, we propose a hybrid multiscale method that combines a fine Monte Carlo simulation on the nodes of interest with a more coarse Langevin dynamics on the rest part. The method is demonstrated to be effective in the Ising model and susceptible-infected-susceptible model.

I. INTRODUCTION

Complex networks have become one of the most active research topics in statistical physics and closely related disciplines.^{1–5} The dynamics of networks and their topologies are usually associated with multiscale processes spanning from microscopic via mesoscopic, to macroscopic level,^{6–8} like human multiscale mobility networks,⁹ module networks,¹⁰ multilayer networks,¹¹ interconnected networks,¹² and networks of networks,¹³ etc. Although computer simulation provides a powerful tool for studying and understanding complex multiscale phenomena, brute-force simulations, such as Monte Carlo (MC) simulation¹⁴ and kinetic MC simulation,¹⁵ are quite expensive and hence computationally prohibited for simulating large networked systems. To the end, some related approaches aimed at speeding

up MC simulations, such as high-performance parallel computing in the classroom using the public goods game as an example.¹⁶ In terms of applicability, effective vaccination and cooperation strategies are also high on the list of applications that would benefit significantly from the speed up.^{17,18} While phenomenological models, such as mean-field description which need much less computational effort, may capture certain properties of the system, but often ignore microscopic and mesoscopic details and fluctuation effects that may be important near critical points. Therefore, a promising way is to develop multiscale theory and approaches, aiming at significantly accelerating the dynamical evolution while properly preserving even microscopic information of interest.

Recently, much efforts have been devoted to developing for coarse graining (CG) approaches. Renormalization transformations have been used to reduce the size of self-similar networks, while preserving the most relevant topological properties of the original ones.^{19–22} Gfeller and Rios proposed a spectral technique to obtain a CG-network which can reproduce the random walk and synchronization dynamics of the original network.^{23,24} Kevrekidis *et al.* developed equation-free multiscale computational methods to accelerate simulation using a coarse time-stepper,²⁵ which has been successfully applied to study the CG dynamics of oscillator networks,²⁶ gene regulatory networks,²⁷ and adaptive epidemic networks.²⁸ Recently, we have proposed a degree-based CG (*d*-CG)²⁹ approach and a strength-based CG (*s*-CG)³⁰ approach to study the critical phenomena of the Ising model, the susceptible-infected-susceptible (SIS) epidemic model, and the *q*-state Potts model on complex networks. However, all these works mentioned above always coarse-grain the whole network. In fact, on the one hand, most real-world networks are very large.³¹ The higher the coarse graining is, the more information is lost. On the other hand, for specific purpose, we often concern the local dynamics of

^{a)}Electronic address: chenhsf@ahu.edu.cn

some nodes of interest other than the entire nodes. Besides, in general, the dynamics of a local part is certainly influenced by that of other parts of the network due to the interactions between connected individuals. Therefore, a natural question arises as to how we simulate a part of interest at a fine level and treat others simultaneously at a CG level, while retaining the microscopic information of interest.

To address the above question, in the present work, we develop a hybrid multiscale coarse-grained (HMCG) method to simulate phase transitions of the networked Ising model and the SIS model, which are often taken as paradigms of equilibrium and non-equilibrium systems, respectively. First, according to the focus of interest, the network is divided into two parts, where the part of interest nodes is named the *core*, and the part of rest ones is called the *periphery*. MC simulations and Langevin equations (LEs) are then performed on the *core* and the *periphery*, respectively. Extensively numerical simulations show that our HMCG method works very well in reproducing the phase diagrams and fluctuations of the microscopic models, while the LE does not. Especially, our HMCG method accelerates the systems' dynamical evolution much more than that of microscopic simulations.

II. HMCG

Without loss of generality, the underlying network is constructed as follows: starting from a random network with N nodes and $N\langle k \rangle/2$ edges, where $\langle k \rangle$ is the average degree. The network is then split into two parts, the *core* consisting of $r_{core}N$ nodes, and the *periphery* with $(1 - r_{core})N$ nodes, where r_{core} denotes the ratio of the number of nodes inside the *core* to that of the entire network. We introduce the parameter u as the density of the inter-edges connecting the two parts, and p_c as the proportion of the number of intra-edges inside the *core* to the total number of intra-edges within both parts. We employ the HMCG method which combines a fine MC simulation with a coarse Langevin dynamics as the fine level method and the CG method to treat the *core* and the *periphery*, respectively.

To account for the idea and procedure of the HMCG method, we give a schematic illustration by a module network consisting of five connected random subgraphs with different topologies, as shown in Fig. 1. The main idea is as follows: to capture the local information and achieve high efficiency in the simulation, the network is divided into two parts, i.e., the *core* which is the module of interest and the *periphery* which consists of the rest ones. Then, a fine level simulation and a CG level one are performed on the part of interest and the other part of rest, respectively. Here, we adopt a microscopic simulation of detailed allowed by classical MC dynamics and a LE to treat the two parts, respectively.

The main steps are summarized below:

- (i) *Identifying the network parts.* According to the requirement of interest, the network is split into two parts, i.e., the *core* and the *periphery*. We then employ \mathcal{C} , \mathcal{P} , and \mathcal{B} to denote the adjacency matrices of intra-*core*, intra-*periphery*, and inter-parts, respectively. Note that \mathcal{P} and \mathcal{B} are coarse grained, while \mathcal{C} preserves so as to pay

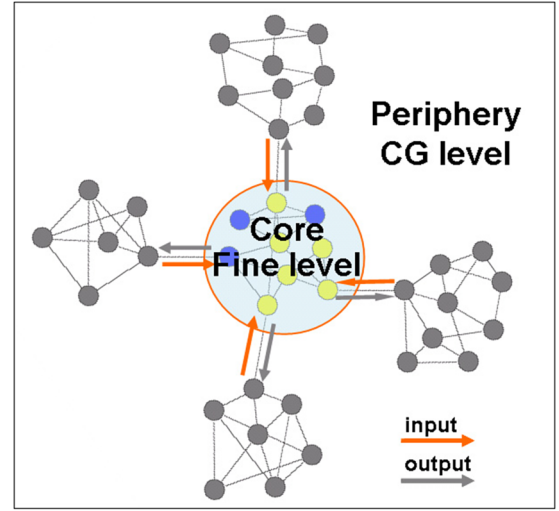


FIG. 1. Schematic illustration of the hybrid multiscale coarse-grained method. The original network is divided into two parts, i.e., the part of module of interest named the *core*, and the part of rest ones named the *periphery*, which are treated at a fine level and a CG level, respectively.

close attention to the part of the original system which is different from other CG methods.

- (ii) *Determining the input and output.* In view of the *core* is the part of interest, we define the flux from the *periphery* to the *core* as the input, where the flux is the product of the mean-field of the *periphery* and the average links between the two parts, and the output is the reverse process.
- (iii) *Performing simulations.* Simulation methods such as MC dynamics, kinetic MC dynamics, molecular dynamics, etc. are performed on the *core* and the *periphery* with a more coarse method, e.g., the LE, spectrum coarse graining, d -CG, s -CG, and other CG methods. Specifically, here, MC simulation and LE are employed as the fine level method and the CG method to treat the part of interest and the rest one, respectively.
- (iv) *Improving the method.* The CPU time of the HM method and that of microscopic MC simulations is counted and compared as well as the accuracy of the results, and then the method is improved by optimizing the algorithm.

A. Application to the Ising model

To evaluate the potential of the HMCG method, we begin with the networked Ising model, a typical example of an equilibrium system. In a given network, each node is endowed with a spin variable s_i that can be either $+1$ (up) or -1 (down). The Hamiltonian of the system is given by

$$H = -J \sum_{i < j} A_{ij} s_i s_j - h \sum_i s_i \quad (s = \pm 1, i, j = 1, \dots, N), \quad (1)$$

where J is the coupling constant and h is the external magnetic field. The elements of the adjacency matrix of the network take $A_{ij} = 1$ if nodes i and j are connected and $A_{ij} = 0$ otherwise. The degree, that is the number of neighboring nodes, of node i is defined as $k_i = \sum_{j=1}^N A_{ij}$.

MC simulations with Glauber dynamics and LE are performed on the *core* and the *periphery*, respectively (see

Appendix A for the details). Generally, with increasing temperature T , the system undergoes a second-order phase transition at the critical value T_c from an ordered state to a disordered one. Figure 2 plots typical time evolutions of the magnetization of core nodes $m_{core} = \sum_{i \in \mathcal{C}} s_i / (r_{core} N)$ for different size r_{core} at $T = 2.5$ (in unit of J/k_B) and $h = 0$. For both HMCG and the microscopic MC simulations, the systems attain the steady states associated with fluctuating noise after transient time. It is clear that they are in good agreement in the steady-state values of m_{core} , as well as their fluctuating amplitudes for both simulation cases at different size r_{core} , while the LE is not.

Furthermore, m_{core} as a function of T obtained from our HMCG method, micro-MC simulations, and LE are plotted in Fig. 3(a). Again, the agreements between HMCG and MC

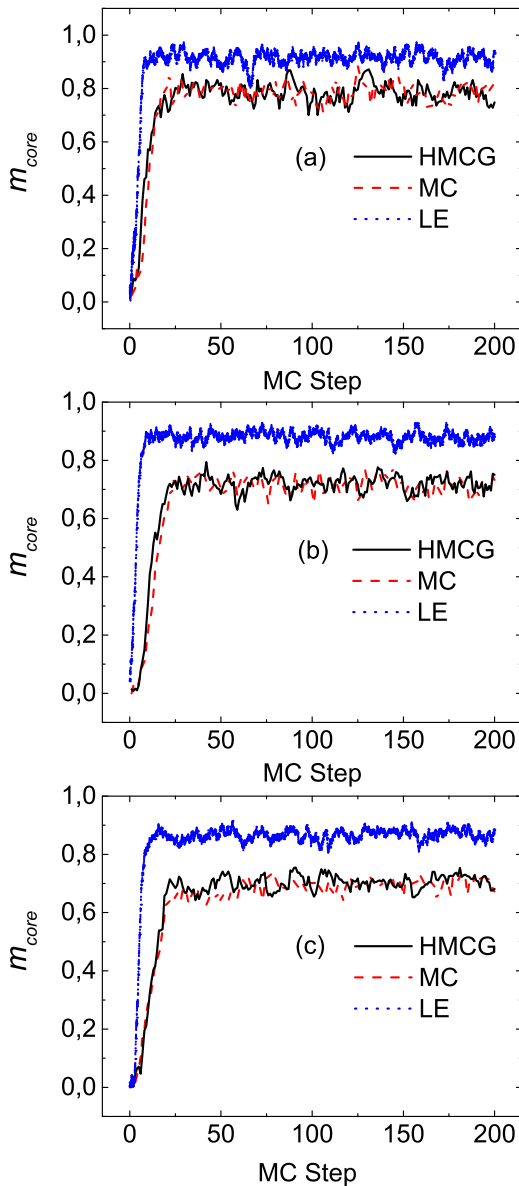


FIG. 2. Typical time evolutions of the magnetization m_{core} in the Ising model at $T = 2.5$ (in unit of J/k_B) and $h = 0$ for (a) $r_{core} = 0.05$, (b) $r_{core} = 0.1$, and (c) $r_{core} = 0.15$, where solid, dashed, and dotted lines indicated HMCG method, MC simulations, and LE approach, respectively. Other parameters are $N = 10000$, $\langle k \rangle = 6$, $u = 0.01$, and $p_c = 0.6$.

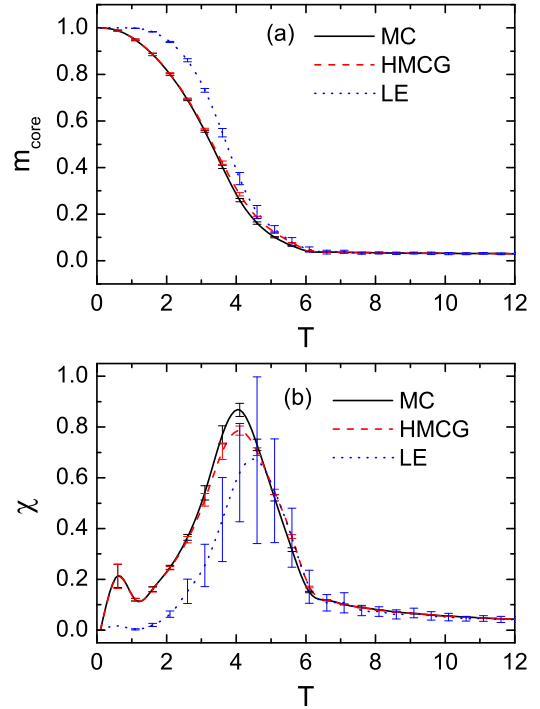
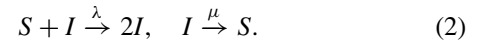


FIG. 3. m_{core} and χ as functions of T for the Ising model on complex networks. The solid, dashed, and dotted lines correspond to the MC, HMCG, and LE simulation results, respectively. The error bars are obtained by averaging over 20 different network realizations. Other parameters are the same as in Fig. 2.

are excellent, further demonstrating the validity of HMCG method. In order to ensure that the microscopic configurations are nearly identical between both methods, we calculate the susceptibility $\chi = r_{core} N (\langle m_{core}^2 \rangle - \langle m_{core} \rangle^2) / (k_B T)$, since χ is related to the variance of the magnetization according to the fluctuation-dissipation theorem, and compare χ as a function of T in Fig. 3(b). Very good agreement is again seen between HMCG and MC methods.

B. Application to the SIS model

Concerning nonequilibrium scenarios, a prototype example is the spreading dynamics of SIS models^{32–34} on the complex network as mentioned above, where individuals inside each node run stochastic infection dynamics as follows:



The first reaction indicates that each susceptible (S) individual with the state variable $\sigma = 0$ becomes infected upon encountering one infected (I) individual with $\sigma = 1$ at a rate λ . The second one reflects that the infected individuals are cured and become again susceptible at a rate μ . For simplicity (yet without loss of generality), we set $\mu = 1$. In this model, a significant and general result is that the system undergoes an absorbing-to-active phase transition at a critical value λ_c with an increasing infectious rate λ .

Our numerical simulation starts from a random configuration with several infected nodes. After an initial transient regime, the system will evolve into a steady state with a constant average density of infected nodes. The steady density of infected nodes ρ is computed by averaging over at least

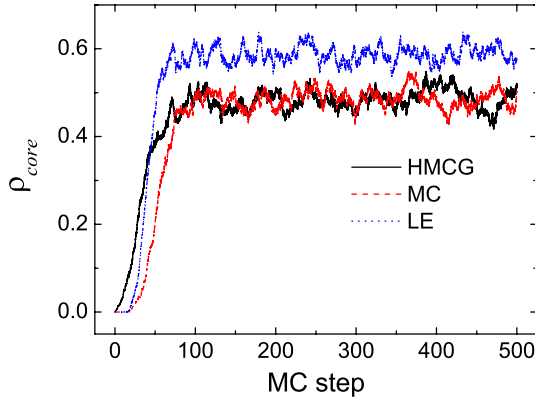


FIG. 4. Typical time evolutions ρ_{core} of the density of infected nodes inside the *core* in the SIS model at $\lambda = 0.8$ for the HMCG method, microscopic MC dynamics, and LE. Other parameters are $N = 10000$, $\langle k \rangle = 6$, $r_{core} = 0.1$, $u = 0.01$, and $p_c = 0.6$.

50 different initial configurations and at least 20 different network realizations for a given λ . Figure 4 compares typical time evolutions $\rho_{core} = \sum_{i \in \mathcal{C}} \sigma_i / (r_{core} N)$ of the density of infected nodes inside the *core* at $\lambda = 0.8$ for the HMCG method, microscopic MC dynamics, and Langevin approach indicated by the solid, dashed, and dotted lines, respectively. Excellent agreement between HMCG and MC is shown.

To further validate the effect of our method, we compare the calculated results of ρ_{core} and normalized susceptibility $\delta = r_{core} N (\langle \rho_{core}^2 \rangle - \langle \rho_{core} \rangle^2) / \langle \rho_{core} \rangle$ as a function of λ in Figs. 5(a) and 5(b), respectively, obtained by the HMCG method, the microscopic MC dynamics, and LE. Clearly,

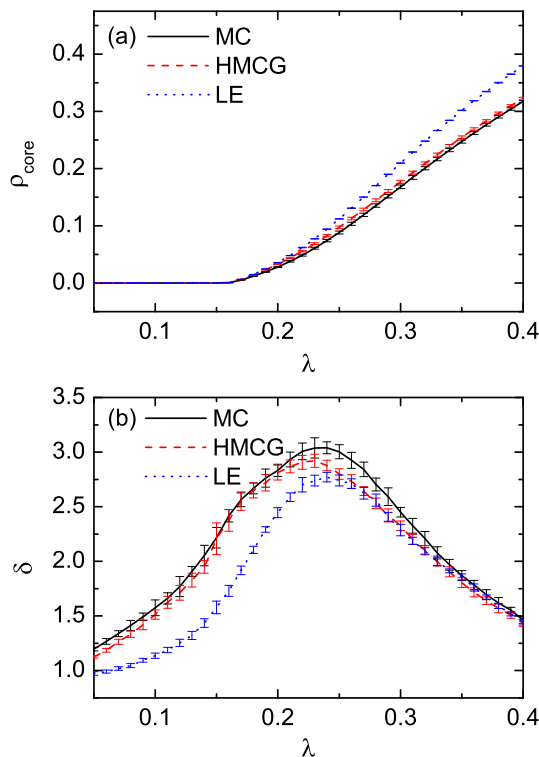


FIG. 5. ρ_{core} and δ as functions of λ for the SIS model on complex networks. The solid, dashed, and dotted lines correspond to the results of MC, HMCG, and LE, respectively. The error bars are obtained by averaging over 20 different network realizations. Other parameters are the same as in Fig. 4.

the agreement between the HMCG and the microscopic MC results remains excellent, while the LE fails. On the one hand, as shown in Fig. 5(a), the HMCG can reproduce well the main characteristic: the system undergoes a phase transition at a certain threshold rate λ_c , above which ρ_{core} monotonically increases from zero indicating the epidemic spreading, otherwise, i.e., $\lambda < \lambda_c$, the system stays in a healthy state with $\rho_{core} = 0$. On the other hand, both HMCG and MC methods exhibit a maximum susceptibility δ at the threshold λ_c , as can be seen in Fig. 5(b), which suggests that the microscopic configurations of the HMCG method are nearly identical to those of the original model. Note that the normalized susceptibility δ adopted here is different from the traditional definition $\delta = r_{core} N (\langle \rho_{core}^2 \rangle - \langle \rho_{core} \rangle^2)$,³⁵ because it leads to clearer numerical results, while preserving all the scaling properties of the usual definition.³⁶

III. DISCUSSION AND CONCLUSIONS

Note that the main goal to develop the multiscale coarse grained method is to improve the computational efficiency. We count the CPU time resulted from microscopic MC simulations and from the HMCG method, indicated by CPU_{MC} and CPU_{HMCG} , respectively, and compare them in Fig. 6(a) for the Ising model and Fig. 6(b) for the SIS model. It can be seen that, on the one hand, the HMCG method provides substantial computational savings compared to the microscopic MC simulations for the same size of network. On the other hand, the ratio CPU_{MC}/CPU_{HMCG} shows an

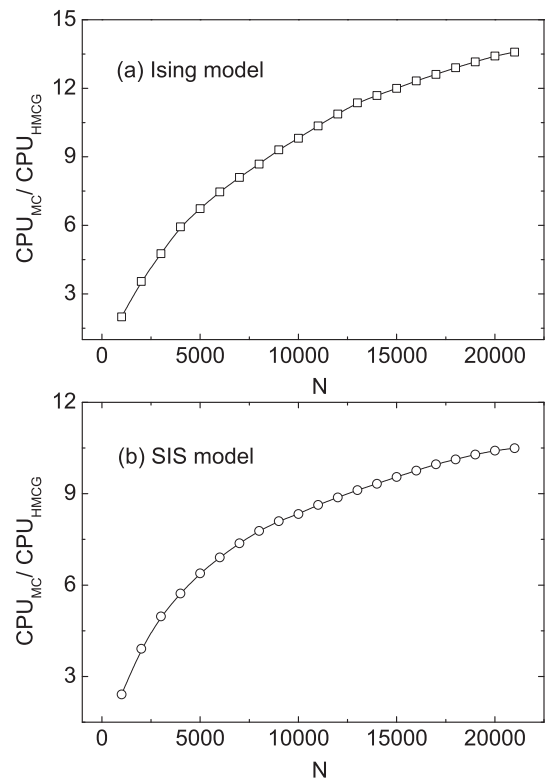


FIG. 6. The proportion CPU_{MC}/CPU_{HMCG} as a function of N for the Ising model (a) and for the SIS model (b), where CPU_{MC} and CPU_{HMCG} denote the CPU time resulted from MC and HMCG methods, respectively. Other parameters in (a) and (b) are the same as in Figs. 2 and 4, respectively.

apparently monotonic dependence on N , suggesting that for a given size of the *core*, the larger the network becomes, the larger the computational savings are. One may approximately estimate the total savings by $CPU_{MC}/CPU_{HMCG} \approx (N \times \langle k \rangle / 2) / (r_{core} N \times \langle k_{core} \rangle / 2 + t_L)$, where $\langle k_{core} \rangle = p_c (1 - u) \langle k \rangle$, denoting the average degree of the group of interest, and t_L denotes the computational cost of LE for the rest group. Generally, $t_L \ll r_{core} N \times \langle k_{core} \rangle / 2$, thus t_L can be neglected and $CPU_{MC}/CPU_{HMCG} \approx 1/[r_{core} \times p_c (1 - u)]$ is obtained. Specifically, for $N = 10\,000$, $\langle k \rangle = 6$, $r_{core} = 0.1$, $u = 0.01$, and $p_c = 0.6$, we obtain $CPU_{MC}/CPU_{HMCG} \approx 16.8$. Obviously, the computational savings are mainly dependent on the relative size of the interest part compared with that of the entire, and on the density of links of intra-*core* and inter-parts. Therefore, if the original network is far larger than the part of interest, the efficiency of our method will become more significant.

In this study, a hybrid multiscale coarse-grained method is proposed that combines a fine simulation for the part of interest with a CG level for the rest of the network. Specifically, microscopic MC simulations and LE are employed to treat both parts, respectively. Extensively numerical simulations demonstrate that both the networked Ising model and SIS model, two paradigms for equilibrium and nonequilibrium systems, show a very good agreement of the HMCG and MC methods. By comparing CPU times for HMCG and MC methods, we find that a large computational cost is saved. The success of our method lies in the accuracy of the mean-field treatment for nodes that we are not interested in. For the networks used in the present work, the nodes are degree-homogeneous and thus the mean-field treatment is valid. However, as such, these periphery nodes are degree-heterogeneous, and, therefore, the simple mean-field treatment becomes invalid. Under such a case, more complex theoretical methods, such as degree-based heterogeneous mean-field treatment, are desirable. The generalization of our method to more complex situations is straightforward. Thus, the proposed method is general, very easy to implement, and directly related to the microscopic models. Therefore, this method can be applied to a wide variety of networked systems just choosing appropriate microscopic simulation methods, such as kinetic MC method, molecular dynamics, and other CG approaches instead of MC method and LE, respectively, in view of different real-world scenarios.

ACKNOWLEDGMENTS

This work was supported by the National Natural Science Foundation of China (NNSFC) (Grant Nos. 11475003, 11875069, and 21473165) and by the National Basic Research Program of China (Grant No. 2013CB834606). C.S. was also funded by the China Scholarship Council (CSC) and the key project of cultivation of leading talents in Universities of Anhui Province (Grant No. gxfzD2016174).

APPENDIX A: DETAILS OF THE HMCG METHOD FOR THE ISING MODEL

The MC simulation at the microscopic level follows standard Glauber dynamics: At each step, we randomly selected

a node from the group of interest nodes and try to flip its spin with an acceptance probability $1/(1 + \exp[\Delta E/(k_B T)])$, where ΔE is the associated change of energy due to the flipping process, k_B the Boltzmann constant, and T the temperature.

A simple recipe of the Glauber algorithm is described as follows:

- (1) Choose an initial state
- (2) Choose a node i at random, $i \in \mathcal{C}$
- (3) Calculate the energy change $\Delta E = \Delta E_{in} + \Delta E_{out}$, resulting from the part of interest and the rest one, respectively, supposed the spin of node i is flipped. Since \mathcal{C} is known for the part of interest, ΔE_{in} can be calculated directly by the microscopic simulations, while ΔE_{out} should be estimated through the mean field coupling between the spin of node i and the net magnetization m' (to be derived in the next step) of the rest part because that \mathcal{P} is coarse grained
- (4) Generate a random number r such that $0 < r < 1$
- (5) If $r < 1/(1 + \exp[\Delta E/(k_B T)])$, flip the spin of node i
- (6) Go to (2)

Next, we will derive the fluctuation-driven LE for m' . The average change of magnetization m' due to spin-flipping can be written as follows:

$$\langle dm' \rangle = dm'_\uparrow \times p_\uparrow \times W_{\uparrow,\downarrow} + dm'_\downarrow \times p_\downarrow \times W_{\downarrow,\uparrow}, \quad (\text{A1})$$

where $dm'_\uparrow = -2/(1 - r_{core})N$ denotes the net change of magnetization if a up-spin turns to down-spin and $dm'_\downarrow = 2/(1 - r_{core})N$ denotes the reverse process. $p_\uparrow = (1 + m')/2$ and $p_\downarrow = (1 - m')/2$ represent the probabilities of up-spins and down-spins, respectively. $W_{\uparrow,\downarrow}$ and $W_{\downarrow,\uparrow}$ represent the transition probabilities from up-spin to down-spin and its reverse process, respectively. According to the rule of Glauber dynamics, they take the forms

$$W_{\uparrow,\downarrow} = \frac{1}{1 + e^{\Delta E'/T}} = \frac{1}{2} \left[1 - \tanh \left(\frac{\Delta E'}{2T} \right) \right], \quad (\text{A2a})$$

$$W_{\downarrow,\uparrow} = \frac{1}{1 + e^{-\Delta E'/T}} = \frac{1}{2} \left[1 + \tanh \left(\frac{\Delta E'}{2T} \right) \right], \quad (\text{A2b})$$

where $\Delta E' = 2(u m' + \sum_{i \in \mathcal{C}} s_i) / (1 - r_{core})N$ is the energy change due to flipping a up-spin within the rest group. Therefore, Eq. (A1) can be rewritten as

$$\langle dm' \rangle = \frac{1}{(1 - r_{core})N} \left[-m' + \tanh \left(\frac{\Delta E'}{2T} \right) \right]. \quad (\text{A3})$$

Then, we calculate the mean square deviation of m'

$$\begin{aligned} \langle dm'^2 \rangle &= \frac{4}{(1 - r_{core})^2 N^2} \times \frac{1 + m'}{2} \times \frac{1}{2} \left[1 - \tanh \left(\frac{\Delta E'}{2T} \right) \right] \\ &\quad + \frac{4}{(1 - r_{core})^2 N^2} \times \frac{1 - m'}{2} \times \frac{1}{2} \left[1 + \tanh \left(\frac{\Delta E'}{2T} \right) \right] \\ &= \frac{1}{(1 - r_{core})^2 N^2} \left[2 - 2m' \tanh \left(\frac{\Delta E'}{2T} \right) \right]. \quad (\text{A4}) \end{aligned}$$

When we adopt $dt = 1/(1 - r_{core})N$, the fluctuation-driven Langevin equation can be obtained

$$\frac{dm'}{dt} = -m' + \tanh\left(\frac{\Delta E'}{2T}\right) + \sqrt{\frac{1}{(1 - r_{core})N} \left[2 - 2m' \tanh\left(\frac{\Delta E'}{2T}\right)\right]} \xi(t), \quad (\text{A5})$$

where $\xi(t)$ is a Gaussian white-noise satisfying $\langle \xi(t) \rangle = 0$ and $\langle \xi(t)\xi(t') \rangle = \delta(t - t')$.

APPENDIX B: DETAILS OF THE HMCg METHOD FOR THE SIS MODEL

To begin, the subgraph of interest is treated with the microscopic MC dynamics as follows:

- (1) Choose an initial state
- (2) Randomly choose a node i , $i \in \mathcal{C}$
- (3) If i is susceptible, calculate the total number of infected individuals nI of its nearest neighbors, which contains within and without the *core*, denoted by nI_{in} and nI_{out} , respectively. Notice that $nI_{in} = \sum_{j \in \mathcal{C}} \mathcal{C}_{ij} \sigma_j$ can be calculated directly by the microscopic simulation, while $nI_{out} = \sum_{j \in \mathcal{P}} \mathcal{P}_{i,j} \sigma_j$ is estimated through the mean field coupling with the average density of infected nodes ρ' inside the rest part, since \mathcal{P} is coarse grained. If i is infectious, go to (6)
- (4) Generate a random number r_1 such that $0 < r_1 < 1$
- (5) If $r_1 < \lambda nI dt$, i is infected, then go to (2)
- (6) Generate a random number r_2 such that $0 < r_2 < 1$
- (7) If $r_2 < dt$, i becomes susceptible, then go to (2)

Then, we will derive the fluctuation-driven LE of ρ' for the rest subgraph. Following Ref. 37, one has

$$\frac{d\rho'}{dt} = -\rho' + \lambda(1 - \rho') \left(\langle k_p \rangle \rho' + \sum_{i \in \mathcal{C}} \mathcal{C} \sigma_i \right) + \sqrt{\frac{1}{(1 - r_{core})N} [\rho' + \lambda(1 - \rho') (\langle k_p \rangle \rho' + \sum_{i \in \mathcal{C}} \mathcal{C} \sigma_i)]} \xi(t), \quad (\text{B1})$$

where $\langle k_p \rangle = (1 - u)(1 - r_{core} p_c) \langle k \rangle / (1 - r_{core})$ denotes the average degree of the subgraph of the rest, σ_i is the state variable of node i , $\sigma_i = 0, 1$ represent susceptible and infectious, respectively. $\xi(t)$ is also a Gaussian white-noise satisfying $\langle \xi(t) \rangle = 0$ and $\langle \xi(t)\xi(t') \rangle = \delta(t - t')$.

¹R. Albert and A.-L. Barabási, *Rev. Mod. Phys.* **74**, 47 (2002).

²S. N. Dorogovtsev and J. F. F. Mendes, *Adv. Phys.* **51**, 1079 (2002).

³S. Boccaletti, V. Latora, Y. Moreno, M. Chavez, and D.-U. Hwang, *Phys. Rep.* **424**, 175 (2006).

⁴A. Arenas, A. Díaz-Guilera, J. Kurths, Y. Moreno, and C. Zhou, *Phys. Rep.* **469**, 93 (2008).

⁵S. N. Dorogovtsev, A. V. Goltsev, and J. F. F. Mendes, *Rev. Mod. Phys.* **80**, 1275 (2008).

⁶Y.-Y. Ahn, J. P. Bagrow, and S. Lehmann, *Nature* **466**, 761 (2010).

⁷M. A. Serrano, M. Boguná, and A. Vespignani, *Proc. Natl. Acad. Sci. U.S.A.* **106**, 6483 (2009).

⁸H. Jang, S. Na, and K. Eom, *J. Chem. Phys.* **131**, 245106 (2009).

⁹D. Balcan, V. Colizza, B. G. Çalves, H. Hu, J. J. Ramasco, and A. Vespignani, *Proc. Natl. Acad. Sci. U.S.A.* **106**, 21484 (2009).

¹⁰M. Girvan and M. E. J. Newman, *Proc. Natl. Acad. Sci. U.S.A.* **99**, 7821 (2002).

¹¹S. Boccaletti, G. Bianconi, R. Criado, C. I. del Genio, J. Gómez-Gardeñes, M. Romance, I. Sendiña Nadal, Z. Wang, and M. Zanin, *Phys. Rep.* **544**, 1 (2014).

¹²M. D. Domenico, A. Solé-Ribalta, S. Gómez, and A. Arenas, *Proc. Natl. Acad. Sci. U.S.A.* **111**, 8351 (2014).

¹³J. Gao, S. V. Buldyrev, H. E. Stanley, and S. Havlin, *Nat. Phys.* **8**, 40 (2012).

¹⁴D. P. Landau and K. Binder, *A Guide to Monte Carlo Simulations in Statistical Physics* (Cambridge University Press, Cambridge, 2000).

¹⁵D. T. Gillespie, *J. Phys. Chem.* **81**, 2340 (1977).

¹⁶M. Perc, *Eur. J. Phys.* **38**, 045801 (2017).

¹⁷Z. Wang, C. T. Bauch, S. Bhattacharyya, A. d'Onofrio, P. Manfredi, M. Perc, N. Perra, M. Salathé, and D. Zhao, *Phys. Rep.* **664**, 1 (2016).

¹⁸M. Perc, J. J. Jordan, D. G. Rand, Z. Wang, S. Boccaletti, and A. Szolnoki, *Phys. Rep.* **687**, 1 (2017).

¹⁹B. J. Kim, *Phys. Rev. Lett.* **93**, 168701 (2004).

²⁰C. Song, S. Havlin, and H. A. Makse, *Nature* **433**, 392 (2005).

²¹K.-I. Goh, G. Salvi, B. Kahng, and D. Kim, *Phys. Rev. Lett.* **96**, 018701 (2006).

²²F. Radicchi, J. J. Ramasco, A. Barrat, and S. Fortunato, *Phys. Rev. Lett.* **101**, 148701 (2008).

²³D. Gfeller and P. D. L. Rios, *Phys. Rev. Lett.* **99**, 038701 (2007).

²⁴D. Gfeller and P. D. L. Rios, *Phys. Rev. Lett.* **100**, 174104 (2008).

²⁵I. G. Kevrekidis, C. W. Gear, J. M. Hyman, P. G. Kevrekidis, O. Runborg, and C. Theodoropoulos, *Commun. Math. Sci.* **1**, 715 (2003).

²⁶S. J. Moon, R. Ghanem, and I. G. Kevrekidis, *Phys. Rev. Lett.* **96**, 144101 (2006).

²⁷R. Erbana, I. G. Kevrekidis, D. Adalsteinsson, and T. C. Elston, *J. Chem. Phys.* **124**, 084106 (2006).

²⁸T. Gross and I. G. Kevrekidis, *Europhys. Lett.* **82**, 38004 (2008).

²⁹H. S. Chen, Z. H. Hou, H. W. Xin, and Y. J. Yan, *Phys. Rev. E* **82**, 011107 (2010).

³⁰C. S. Shen, H. S. Chen, Z. H. Hou, and H. W. Xin, *Phys. Rev. E* **83**, 066109 (2011).

³¹M. I. Rabinovich, P. Varona, A. I. Selverston, and H. D. I. Abarbanel, *Rev. Mod. Phys.* **78**, 1213 (2006).

³²R. Anderson and R. M. May, *Infectious Diseases in Humans* (Oxford University Press, Oxford, 1992).

³³D. J. Daley and J. Gani, *Epidemic Modelling* (Cambridge University Press, Cambridge, 1999).

³⁴R. Pastor-Satorras, C. Castellano, P. Van Mieghem, and A. Vespignani, *Rev. Mod. Phys.* **87**, 925 (2015).

³⁵J. Marro and R. Dickman, *Nonequilibrium Phase Transitions in Lattice Models* (Cambridge University Press, Cambridge, 1999).

³⁶S. C. Ferreira, C. Castellano, and R. Pastor-Satorras, *Phys. Rev. E* **86**, 041125 (2012).

³⁷M. Boguñá, C. Castellano, and R. Pastor-Satorras, *Phys. Rev. E* **79**, 036110 (2009).